A Methodology for Instantaneous Polarization Measurements Using a Calibrated Dual-Polarized Probe

Brett T. Walkenhorst, Steve Nichols
NSI-MI Technologies
Suwanee, GA 30024
bwalkenhorst@nsi-mi.com
snichols@nsi-mi.com

Abstract - Accurately measuring the polarization of an antenna is a topic that has garnered much interest over many years. Methods abound including phase-referenced measurements using two orthogonal polarizations, phase-less measurements using two or three pairs of orthogonal polarizations, spinning linear probe measurements, and the rigorous three-antenna polarization method. In spite of the many publications on the topic, polarization measurements are very challenging and can easily lead to confusion, particularly in accurately determining the sense of polarization.

In this paper, we describe a method of accurately and rapidly measuring the polarization of an antenna with the aid of a multi-channel measurement receiver and a dual-polarized probe. The method acquires phase-referenced measurements of two orthogonal polarizations. To enable such measurements, we describe a methodology for calibrating the probe. We also describe a tool for automating the polarization measurement and display of the polarization state. By automating the process, it is hoped that the common challenges and confusions associated with polarization measurements may be largely obviated.

Keywords—Polarization, Dual-polarized probe, Calibration, Antenna measurements

I. INTRODUCTION

Several polarization measurement techniques are described in [1] and [2], and most are still in use today.In its simplest form, axial ratio can be obtained by inspecting the pattern produced when a linearly polarized probe is rotated one full revolution with respect to an antenna under test (AUT). The ratio of the peak power to minimum power across the pattern yields the axial ratio. The tilt angle can also be determined from the physical location of the peaks and nulls. This technique works best when measuring nominally linearly polarized antennas. For nominally circularly polarized antennas, the axial ratio may readily be observed by scanning the AUT while simultaneously rotating a linearly polarized probe at a rapid speed. The higher frequency variation in the resulting amplitude pattern can be observed as the axial ratio. None of these pattern analysis techniques require a phase measurement, but they also do not determine the polarization sense.

Polarization methods that require complex phase and amplitude measurements can fully characterize the polarization state, including the sense. The three-antenna method enables determination of the complex polarization ratio as well as gain for three arbitrary antennas [3-5]. Variations of this method have been proposed to improve accuracy and repeatability, especially for measuring antennas with a high axial ratio [6-7].

Measurement of polarization using orthogonal components can be accomplished with a single linearly polarized probe installed on a rotation stage. With the probe oriented at 0 and 90 degrees, two orthogonal complex polarization measurements can be made. These can be used to determine the complex polarization ratio, axial ratio, tilt angle, and sense. This technique is also commonly used in near-field measurement systems.

In a desire to speed up such measurements, dual linearly polarized probes were introduced [8]. For accurate measurements, calibration to a known linear standard is required, such as a waveguide probe or standard gain horn. Adjustments must also be made for channel imbalance in the RF paths for two probe ports, which often includes an RF switch. As broad band dual-polarized probes have been developed (e.g. [9]), techniques have been refined to compensate for both channel imbalance and polarization distortion [10-14].

Further advancements are described in this paper. In our measurement system, the RF switch that selects between the two ports of the dual-polarized probe has been eliminated. Instead, a multi-channel measurement receiver, the NSI-MI Vector Field Analyzer, is used to simultaneously measure both ports of the probe (Figure 1). This also eliminates the disparity in time between the two orthogonal polarization measurements that occurs when using an RF switch.

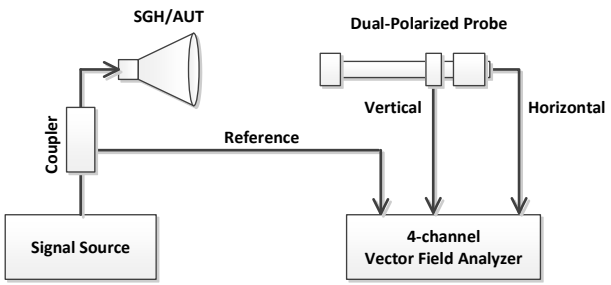

Figure 1. Polarization Measurement System

Based on this system, a new polarization measurement tool has been developed. It simplifies the calibration process by using graphical diagrams of the calibration standard and probe orientations as they are installed in the system. The user simply selects the correct diagram for what is observed from the range perspective. After calibration, the calibration standard is replaced by the AUT. On command, the polarization measurement tool acquires the two orthogonal polarization components from the Vector Field Analyzer. Polarization parameters for the AUT are calculated and displayed immediately, including the polarization ellipse, axial ratio, tilt angle, and sense. The tool can loop indefinitely, providing a real-time update as adjustments or alignment procedures are performed.

This tool is described in Section IV. To lay the proper foundation, we offer a brief overview of polarization theory in Section II and describe the calibration procedure of the dual-polarized probe, as implemented by the tool, in Section III. Conclusions are summarized in Section V.

II. Polarization Theory

The electric field of a single-frequency propagating plane wave may be written as [15]

$$\vec{E}(\vec{x},t) = (E_1\hat{e}_1 + E_2\hat{e}_2)e^{j(\omega t - \vec{k}\cdot\vec{x})} \quad (1)$$

Here, E_1 and E_2 are complex projections of the field onto two polarization bases at some point in time and space where $\omega t = \vec{k}\cdot\vec{x}$. In general, these bases can be any set of orthogonal pairs, but for convenience, we will let E_1 indicate horizontal polarization and E_2 vertical. And again, for convenience, we will let the direction of propagation be along the z-axis in the positive direction. Given these assumptions ($\hat{e}_1 = \hat{e}_x$, $\hat{e}_2 = \hat{e}_y$, $\vec{x} = z\hat{e}_z$, and $\vec{k} = k\hat{e}_z$), we can rewrite the E-field as

$$\vec{E}(z,t) = \left(E_1\hat{e}_x + E_2\hat{e}_y\right)e^{j(\omega t - kz)} \quad (2)$$

We can write the projected fields generically as

$$E_1 = a_1 e^{j\phi_1} \quad (3)$$

$$E_2 = a_2 e^{j\phi_2} \quad (4)$$

where a_1 and a_2 represent the magnitudes and ϕ_1 and ϕ_2 the phases of the two field components.

We can then write the field components of the wave as follows

$$E_x(z,t) = \mathcal{R}e\{\vec{E}(z,t)\cdot\hat{e}_x\} = \mathcal{R}e\{E_1 e^{j(\omega t - kz)}\} = a_1\cos(\omega t - kz + \phi_1) \quad (5)$$

$$E_y(z,t) = \mathcal{R}e\{\vec{E}(z,t)\cdot\hat{e}_y\} = \mathcal{R}e\{E_2 e^{j(\omega t - kz)}\} = a_2\cos(\omega t - kz + \phi_2) \quad (6)$$

At a fixed point in space along the z-axis, z_0, if we let t vary over an interval of time equal to λ/c, the tip of the field vector will trace an ellipse as the wave propagates through the plane defined by $z = z_0$. Here λ is the wavelength of the single-frequency wave and c is the speed of the propagating wave. Thus, we let time progress until one wavelength has passed through the plane defined by $z = z_0$.

Figure 2 below shows an example of such an ellipse, traced by a wave whose polarization is defined by $E_1 = 1$ and $E_2 = 0.6e^{j(0.4\pi)}$, with positive z-axis pointing toward the reader.

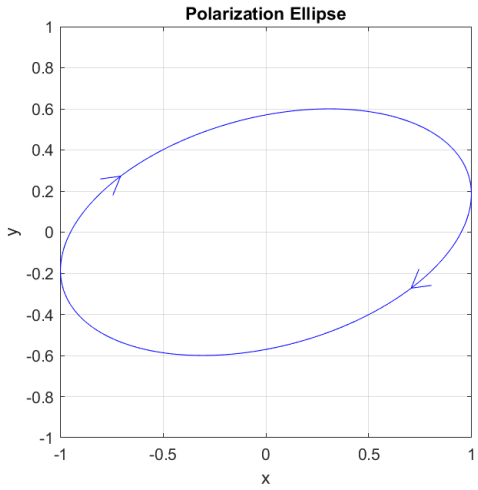

Figure 2. Polarization ellipse associated with $E_1 = 1$ and $E_2 = 0.6e^{j(0.4\pi)}$ (left-handed sense)

Figure 3 shows a 3-D plot of the same wave at a single point in time. The spiral indicates the location of the stationary field at various points in space. The z-axis, indicated by the large arrow in the center of the diagram, is scaled in units of wavelengths. The field vectors, some of which are indicated on the figure with arrows pointing from the z-axis toward the spiral, are the vectors computed from the field components in (5) and (6) at various values of z for $t = 0$. The single field vector passing through the plane $z = \lambda$ is highlighted.

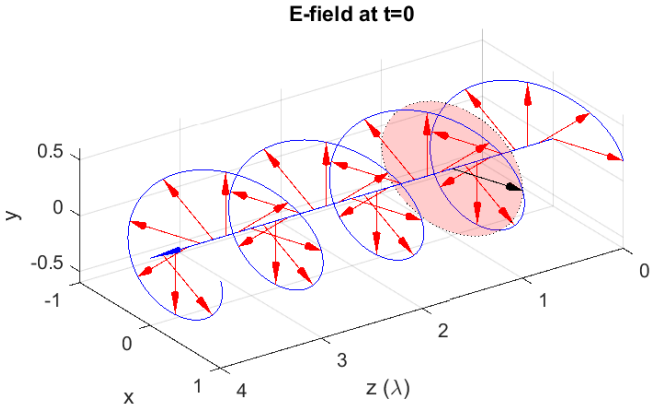

Figure 3. Three-dimensional wave representation for $E_1 = 1$ and $E_2 = 0.6e^{j(0.4\pi)}$ at time t=0 (left-handed sense)

As time progresses, the wave propagates in the positive z direction, and the field vectors translate along the axis of propagation. Although the field vectors may appear to be rotating given the helical nature of the field vectors in space, a careful examination of the equations shows that they are fixed

in orientation when launched from the antenna's aperture and simply translate along the direction of the propagation vector. The perception of rotation occurs as the field vectors pass through a fixed z-plane over time. The highlighted cross-section at $z = \lambda$ indicates a slice of space where a polarization ellipse is traced over time. In this example, the field at $z = \lambda$ rotates clockwise as shown in Figure 2, indicating a left-handed polarized wave.

III. Probe Calibration

In this section, we will discuss the calibration of a dual-polarized probe for accurate polarization state measurements. The procedure here makes some assumptions in order to quickly calibrate the probe. As such, this method will not be as accurate as the three-antenna method for measuring polarization [6], but it can offer a quick snapshot of reasonably accurate fidelity to give the user a good idea of polarization state of an AUT.

Our first assumption is that we have access to an antenna that can act as a standard for polarization. We recommend using standard gain horns (SGH), which typically have very pure polarization characteristics. We use the standard to calibrate for the polarization response of the dual-polarized probe including any feed network, multiplexer, cables, etc. Note that the calibration is highly sensitive to changes in the feed network, cable length, permittivity, etc. Calibration should be performed every time the feed network is changed, including the disconnection and reconnection of cables within the feed network, even if the same cable is reconnected. Failure to do so will degrade the accuracy of the calibration data.

After mounting the SGH in the AUT position, the user should make reasonable efforts to align the antenna along the range axis and should very carefully align the polarization vector of the SGH relative to gravity using a level placed against the side wall of the horn.

With the SGH horizontally polarized and feed port pointing in the positive x-direction of the AUT coordinate system (pointing right when we're looking into the face of the SGH), we collect a Jones vector using the dual-polarized probe. This configuration is represented graphically in Figure 4 (probe orientation) and Figure 5 (SGH orientation). Note we assume an AUT coordinate system of $(\hat{x}, \hat{y}, \hat{z})$ and a probe coordinate system of $(\hat{x}_p, \hat{y}_p, \hat{z}_p)$.

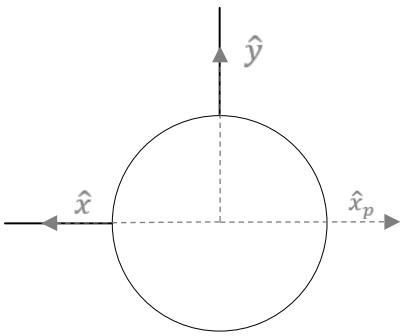

Figure 4. Orientation of dual-polarized probe for calibration

The resultant Jones vector represents the polarization state of the H-pol wave from the perspective of the probe. With the probe oriented such that its vertical port points up and its horizontal port points to the left when looking into the face of the aperture, we call the probe's H-port response to this wave $E_{H,CP}$ and the probe's V-port response to this wave $E_{H,XP}$. Note we are trusting the polarization of the SGH to be purely H-pol, so we use notation to that effect. Each of these is a complex value, so phase-referenced measurements must be made.

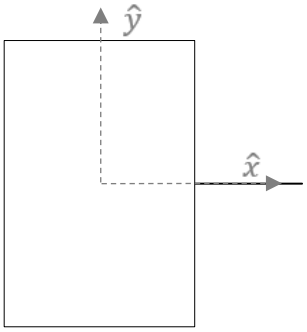

Figure 5. Orientation of SGH for H-pol calibration

We now rotate the SGH so that it's vertically polarized, with the feed port pointing in the positive y-direction (pointing up) and collect another Jones vector using the dual-polarized probe. This configuration is represented graphically in Figure 6. The resultant Jones vector represents the polarization state of the V-pol wave from the perspective of the probe. With the probe oriented such that its vertical port points up and its horizontal port points to the left when looking into the face of the aperture, we call the probe's H-port response to this wave $E_{V,XP}$ and the probe's V-port response to this wave $E_{V,CP}$.

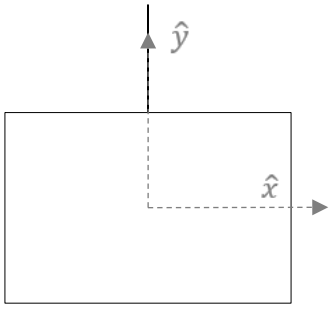

Figure 6. Orientation of SGH for V-pol calibration

It isn't strictly necessary to collect the data in the orientations described and pictured above. If the orientation of one of the ports is in the opposite direction from what is specified, we can simply negate the measured result to simulate the effect of rotating the SGH or probe 180 degrees. We can also use this trick to average two to four measurements with different combinations of SGH and probe orientations. This may help somewhat to minimize the effect of room reflections [12].

A single-reflector compact antenna test range (CATR) will reverse the x-axis relative to a near-field or far-field

configuration as the wave reflects off the paraboloidal reflector. Thus, when looking into the aperture of the dual-polarized feed antenna, the direction of the port along the x-axis should be opposite that of the configuration shown in Figure 5 and 6 above. This reversed configuration for a CATR is shown in Figure 7. Once again, we can handle other orientations by simply negating the response of that port.

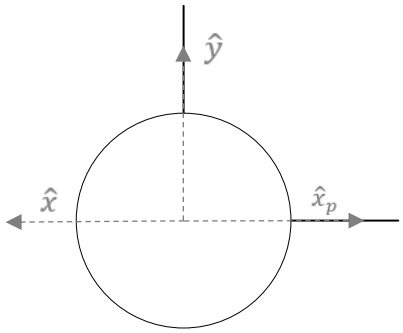

Figure 7. Orientation of dual-polarized CATR feed

Having collected a Jones vector for an H-pol wave and a Jones vector for a V-pol wave, we can now stack these Jones vectors side by side to form a Jones matrix. This matrix represents the transformation from the polarization bases of the SGH (which we assume to be purely H- and V-polarized) to the polarization bases of the probe (including its feed network, cables, switches, etc.). That Jones matrix has the form

$$J = \begin{pmatrix} E_{H,CP} & E_{V,XP} \\ E_{H,XP} & E_{V,CP} \end{pmatrix} \tag{7}$$

For each element of the matrix, we assume the H-port of both probe and SGH point in the $+\hat{x} = -\hat{x}_p$ direction and the V-port of both probe and SGH point in the $+\hat{y} = +\hat{y}_p$ direction. The following table summarizes the four elements of the Jones matrix in terms of antenna pair orientations.

Jones matrix element	Probe port orientation	SGH port orientation
$E_{H,CP}$	H-pol	H-pol
$E_{H,XP}$	V-pol	H-pol
$E_{V,XP}$	H-pol	V-pol
$E_{V,CP}$	V-pol	V-pol

If we denote pure H-pol as E_H, pure V-pol as E_V, and the probe's nominal H-pol and V-pol states as $\tilde{E}_H$ and $\tilde{E}_V$, respectively, we can write the coupling equation as

$$\begin{pmatrix} \tilde{E}_H \\ \tilde{E}_V \end{pmatrix} = \begin{pmatrix} E_{H,CP} & E_{V,XP} \\ E_{H,XP} & E_{V,CP} \end{pmatrix} \begin{pmatrix} E_H \\ E_V \end{pmatrix} \tag{8}$$

Now that we have this Jones matrix, we know how to convert from one set of bases to another. This means that for any acquisition we make with the dual-polarized probe, as long as we don't change its configuration and perturb the Jones matrix, we now have the information needed to transform from the probe's polarization bases to the polarization bases of the SGH, which we assume to be very pure. Note that it is critical to carefully align the SGH's walls with gravity so that we aren't unintentionally introducing some tilt into the polarization vector when we make our calibration measurements.

At this point, we introduce our second assumption. In transforming from one set of bases to another, we are implicitly assuming that what we measure in the calibration step to create our Jones matrix includes only the coupling coefficients between our antennas. But in reality, it will include other effects, most notably room reflections. These will perturb the Jones matrix and introduce error, so it is strongly recommended to make the calibration and subsequent test measurements in a properly treated anechoic chamber to minimize the effect of this error.

To perform our transformation, we simply need to invert the Jones matrix and apply it to all measurements of the dual-polarized probe. However, to avoid normalizing the post-transformed signals relative to the inputs, we preserve the magnitude of the first port to allow us to fix the energy of the transformation for at least one port. We can't do this for both ports simultaneously because we are mixing power levels of co- and x-pol terms when we transform polarization bases, so we must pick one port whose energy we wish to preserve. Thus, we write our transformation matrix as

$$\begin{aligned} T &= E_{H,CP} J^{-1} \\ &= \frac{E_{H,CP}}{E_{H,CP}E_{V,CP} - E_{V,XP}E_{H,XP}} \begin{pmatrix} E_{V,CP} & -E_{V,XP} \\ -E_{H,XP} & E_{H,CP} \end{pmatrix} \end{aligned} \tag{9}$$

When this transformation matrix is applied to the probe's response to the SGH, we obtain

$$T \begin{pmatrix} \tilde{E}_H \\ \tilde{E}_V \end{pmatrix} = T \begin{pmatrix} E_{H,CP} & E_{V,XP} \\ E_{H,XP} & E_{V,CP} \end{pmatrix} \begin{pmatrix} E_H \\ E_V \end{pmatrix} = E_{H,CP} \begin{pmatrix} E_H \\ E_V \end{pmatrix} \tag{10}$$

which is the Jones vector of the SGH when rotated in two different orientations. When we apply this transformation matrix to data obtained with the dual-polarized probe, this is analogous to taking that data with an SGH in those two orientations.

IV. Polarization Measurement Tool

The methodology appears straight forward, but there are several places where one can invert a convention, making it difficult to perform the method correctly without some form of automation. Inverting one of the fields typically has the effect of inverting the sense of the polarization state. This may not be critical when measuring antennas that are nominally linearly polarized, but it can disruptive, if not catastrophic, when measuring antennas that are nominally circularly polarized.

It is therefore advisable to employ a tool for automating the process. The use of such a tool with a Vector Field Analyzer and a dual-polarized probe also enables instantaneous measurements of polarization state over multiple frequencies for a given aspect angle. This section describes such a tool.

The first step in the method is to calibrate the probe. In order to do this, we must know the orientation of the probe and

the way it is cabled. The tool allows the user to select these with simple graphics to ensure that the correct conventions are employed. The tool will then transform the data to a common convention as described in Section III. This selection is shown in Figure 8. An option also exists to tell the tool that the probe is actually a feed in a compact range. The tool would then invert the horizontal component to accommodate that configuration.

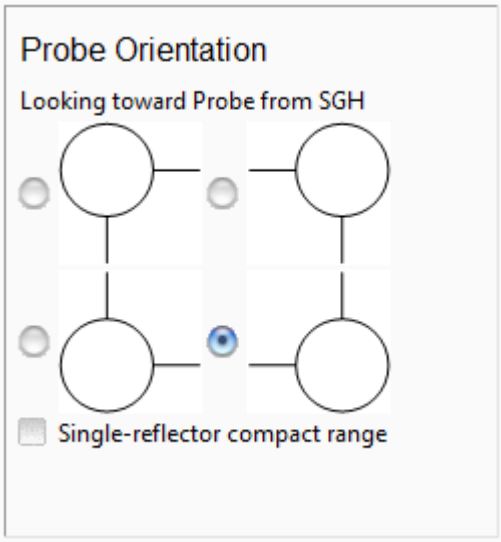

Figure 8. Selection of probe orientation in polarization measurement tool

The cabling of the probe is also selectable, allowing a user to connect the cables in whatever order is convenient and then telling the tool which channel belongs to which port. This portion of the tool is shown graphically in Figure 9. In the figure, we see that channel A is connected to the horizontal port while channel B is connected to the vertical port. The tool will re-order channels as necessary to ensure a common convention for the collected Jones vectors.

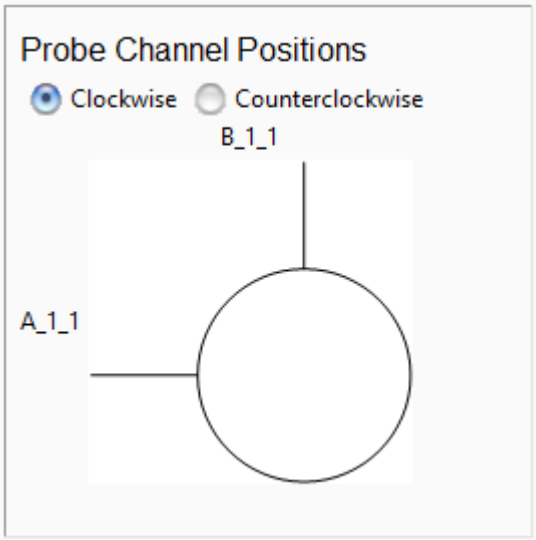

Figure 9. Selection of probe cabling in polarization measurement tool

Once the correct probe orientation has been selected, calibration data can be collected using one or both orientations of vertical and horizontal SGH polarizations. At least one vertical and one horizontal Jones vector must exist in order to generate a complete calibration file. This capability is shown graphically in Figure 10. The user simply pushes a button to collect data, but the button chosen must correspond to the orientation of the SGH. The tool automates the collection by communicating directly with the Vector Field Analyzer and storing the calibration data in memory.

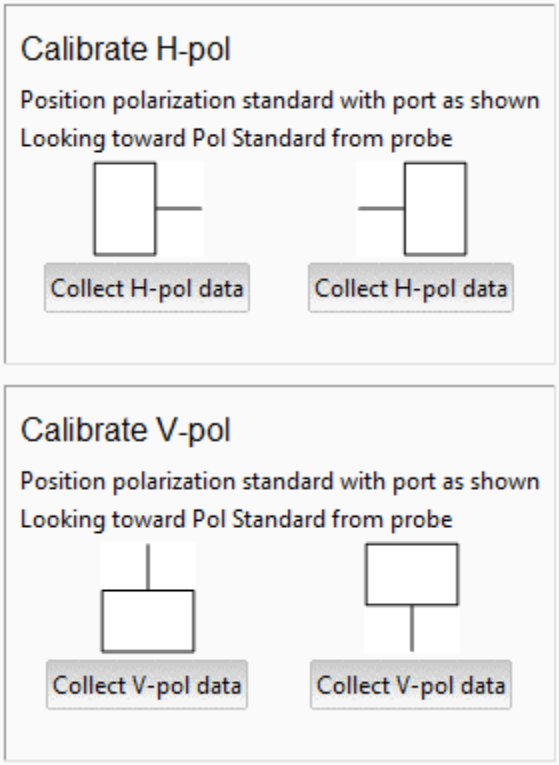

Figure 10. Calibration data acquisition panel in polarization measurement tool

After calibration data has been acquired, multi-channel data can be collected on an arbitrary AUT. The calibration data can be applied if desired, as controlled by the user. The user may also select a frequency among the list of frequencies acquired for plotting purposes. These controls are shown in Figure 11.

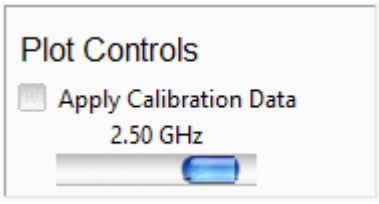

Figure 11. Plot control panel in polarization measurement tool

Having collected complete polarization information using a calibrated dual-polarized probe, we can now plot the polarization information any way we choose. The tool can

automate the plotting of axial ratio, tilt, and sense. The plotted tilt angles for a sinuous antenna [13] are shown in Figure 12.

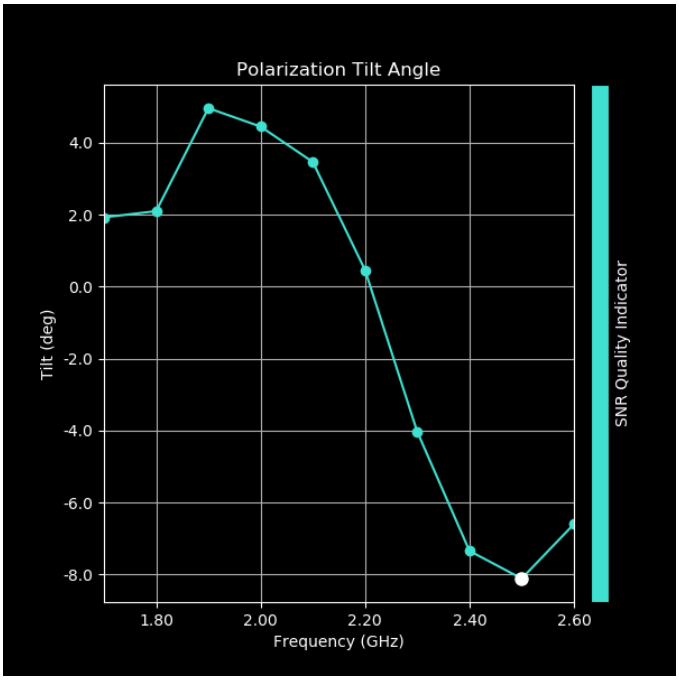

Figure 12. Tilt angle of a sinuous antenna displayed in polarization measurement tool

The tool can also plot the polarization ellipse for a single frequency as described in Section II. The polarization ellipse for the sinuous antenna at 2.5 GHz is shown in Figure 13.

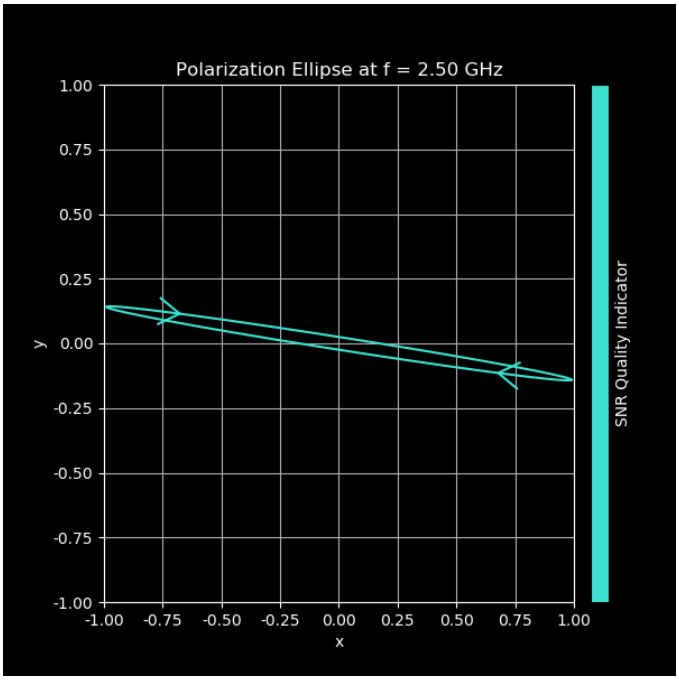

Figure 13. Polarization ellipse of a sinuous antenna at 2.5 GHz displayed in polarization measurement tool

V. Conclusions

A methodology has been developed for making instantaneous measurements of the polarization of an antenna using a dual-polarized probe and a multi-channel measurement receiver. The methodology includes the calibration of the probe and a transformation of polarization bases to yield accurate polarization state information of an arbitrary antenna. A tool has also been described to automate the measurement process including the display of polarization information in the form of axial ratio, tilt, sense, and/or the polarization ellipse.

References

[1] J.S. Hollis, T.J. Lyon, L. Clayton, *Microwave Antenna Measurements, 3rd edition*. Atlanta: Scientific-Atlanta, Inc., 1985.

[2] R. Heaton. "Antenna Polarization Measurements", in *AMTA Proceedings*, Nov. 1979.

[3] E. B. Joy. "Spatial sampling and filtering in near-field measurements", Ph.D. dissertation, Ga. Inst. of Technology, Atlanta, Nov. 1970.

[4] A. C. Newell and D. M. Kerns. "Determination of both polarization and power gain of antennas by a generalized 3-antenna measurement method", in *Electronic Letters*, vol. 7, pp. 68-70, Feb. 1971.

[5] E. B. Joy and D. T. Paris. "A Practical Method for Measuring the Complex Polarization Ratio of Arbitrary Antennas", in *IEEE Transactions on Antennas and Propagation*, vol. 21, no. 4, pp. 432-435, July 1973.

[6] A. C. Newell. "Improved Polarization Measurements Using a Modified Three-Antenna Technique", in *IEEE Transactions on Antennas and Propagation*, vol. 36, no. 6, pp. 852-854, June 1988.

[7] D. A. Thompson. "A Modified Three-Antenna Polarization Measurement Technique Using a Least-Squares Curve Fit", in *AMTA Proceedings*, Nov. 2005.

[8] G. B. Melson, J. J. Anderson, "A Method for Making Fast High Accuracy Polarization Measurements", *AMTA Proceedings*, Nov. 1986.

[9] L. J. Foged, L. Duchesne, L.Roux, P. Garreau. "Wide-band dual polarized probes for high precision near-field measurements", *AMTA Proceedings*, Nov. 2002.

[10] A. Newell, P. Pelland. "Measuring Low Cross Polarization Using a Broad Band, Log Periodic Probe", in *AMTA Proceedings*, Nov. 2012.

[11] P. Pelland, A. Newell. "Measuring Accurate Low Cross Polarization Using Broad Band, Dual Polarized Probes", in *AMTA Proceedings*, Oct. 2013

[12] P. Pelland, A. Newell. "Combining Pattern, Polarization and Channel Balance Correction Routines to Improve the Performance of Broad Band, Dual Polarized Probes", in *AMTA Proceedings*, Nov. 2014.

[13] B.T. Walkenhorst, D. Tammen, "Correcting polarization distortion in a compact range feed," *Antenna Measurement Techniques Association (AMTA) Symposium*, Nov 2016.

[14] C. Parini, S. Gregson, J. McCormick, D. Janse van Rensburg. Ch. 10.2.2 "Channel-balance correction for antenna measurements", in *Theory and Practice of Modern Antenna Range Measurements*, London: IET, 2015, pp. 538-545

[15] J.D. Jackson, *Classical Electrodynamics, Third Edition*. New York: John Wiley & Sons, 1999, p. 299.